buildings

MDPI

Article

Performance of Geopolymer Mortar Containing PVC Plastic Waste from Bottle Labels at Normal and Elevated Temperatures

Ronnakrit Kunthawatwong [1], Ampol Wongsa [1], Jindarat Ekprasert [2], Piti Sukontasukkul [3], Vanchai Sata [1,*] and Prinya Chindaprasirt [1,4]

[1] Sustainable Infrastructure Research and Development Center, Department of Civil Engineering, Faculty of Engineering, Khon Kaen University, Khon Kaen 40002, Thailand; boomza_14757@hotmail.com (R.K.); ampowo@kku.ac.th (A.W.); prinya@kku.ac.th (P.C.)
[2] Department of Microbiology, Faculty of Science, Khon Kaen University, Khon Kaen 40002, Thailand; jindaek@kku.ac.th
[3] Construction and Building Materials Research Center, Department of Civil Engineering, Faculty of Engineering, King Mongkut's University of Technology North Bangkok, Bangkok 10800, Thailand; piti.s@eng.kmutnb.ac.th
[4] Academy of Science, Royal Society of Thailand, Bangkok 10300, Thailand
* Correspondence: vancsa@kku.ac.th

Abstract: This work focused on reusing polyvinyl chloride (PVC) plastic waste from bottle labels (BLWA) as lightweight aggregates in geopolymer mortar. This way of reusing plastic waste is beneficial for diminishing the negative impacts of plastics on the environment and reducing CO_2 emissions by using geopolymer as an alternative cementing material. BLWA was used to partially substitute natural fine aggregate at ratios of 0, 5, 10, 15, and 20% by volume. The geopolymer mortar properties were tested, and the durability after exposure to elevated temperatures was also assessed. It was found that the strengths were adversely affected by increasing BLWA content. The water absorption and porosity were also increased with beneficial benefits on the reduced density (9–17%) and thermal conductivity (28–44%). The geopolymer mortar containing 5–15% BLWA satisfied the requirement of a lightweight mortar used in masonry work. After exposure to temperatures up to 600 °C, the properties of geopolymer mortar containing BLWA reduced more than that of the control mortar due to the thermal degradation of BLWA at high temperatures. However, when increasing the temperature from 600 °C to 900 °C, there was no further loss in strength. Microstructure analysis indicated that increasing temperatures caused more increased voids and microcracks in geopolymer mortars, especially the ones containing BLWA. However, after exposure at 900 °C, these voids and cracks were minimized at 900 °C due to sintering effects. The findings in this work confirmed the feasibility of using this PVC waste derived to produce lightweight construction material with thermal insulation properties.

Keywords: waste; recycled aggregate; mortar; geopolymer; thermal conductivity

Citation: Kunthawatwong, R.; Wongsa, A.; Ekprasert, J.; Sukontasukkul, P.; Sata, V.; Chindaprasirt, P. Performance of Geopolymer Mortar Containing PVC Plastic Waste from Bottle Labels at Normal and Elevated Temperatures. *Buildings* **2023**, *13*, 1031. https://doi.org/10.3390/buildings13041031

Academic Editor: Pavel Reiterman

Received: 10 March 2023
Revised: 11 April 2023
Accepted: 12 April 2023
Published: 14 April 2023

1. Introduction

Population growth has led to increased consumption of various resources, including plastics. Over five decades, global production of plastics has grown exponentially from 15 to 322 metric tons representing more than 200 times increment [1,2]. The extensive manufacture and consumption of plastic products inevitably result in a large amount of plastic waste. According to the United States Environmental Protection Agency (EPA) report in 2019, only 8.4 percent of plastic waste is recycled, while most of them are left unattended in the environment and discarded in landfills [3]. Some plastic wastes are dumped into the ocean instead of landfill due to the high cost of landfilling [4]. This causes a massive accumulation of plastic waste in the oceans and directly disrupts the livelihoods of marine life. In addition, toxic substances from manufacturing processes,

such as initiators, plasticizers, and flame retardants, are leached out [5–8], which are also harmful to many aquatic creatures. Another major concern is that plastic wastes can be decomposed into microplastic, the most detrimental form of plastics, through abrasion, weather changes, or exposure to ultraviolet radiation from sunlight [9]. Therefore, plastic waste can have a serious impact on the environment and the well-being of many lives. To reduce such negative impacts, the incorporation of plastic wastes into engineering materials then becomes one of the promising ways to immobilize and reuse these wastes.

Concrete consists mostly of aggregates. Therefore, massive amounts of aggregates are used for concrete production, which could reach 47.5 billion tons globally by 2023 [10]. In addition to reducing natural resource consumption, the substitution of conventional aggregate with recycled aggregate can also reduce waste. Celik et al. [11] investigated the properties of concrete replaced fine and coarse aggregate with a crushed waste glass of 0, 10, 20, 30, 40, and 50%. The results showed that the compressive, flexural, and splitting tensile strength of concrete increased with an increase in fine aggregate replacement. While using waste glass as coarse aggregate, the mechanical properties of concrete showed a decreased value. By using the numerical analysis of data collected from previous research, Basaran et al. [12] reported that by replacing sand with up to 15% marble aggregate, the compressive strength of concrete increased in the range of 2–26%.

Among various types of plastics used nowadays, polyethylene terephthalate (PET) waste derived from plastic bottles has been one of the most widely studied plastics for application as aggregates in engineering materials [13–16]. However, what has been overlooked is that most plastic bottles have plastic labels, which are usually made of polyvinyl chloride (PVC). To date, there is still no proper way to effectively manage and recycle these PVC wastes, resulting in more environmental problems. Therefore, it is important to find alternative applications for reusing these wastes.

Recently, the reduction of plastic wastes by incorporating them as aggregates in cement materials has been widely investigated. For example, Boucedra et al. [17] tested the replacement of natural fine aggregates with plastic at ratios of 0, 25, 50, and 75% by volume in concrete. The results revealed that the compressive strength of concrete reduced with increasing content of plastic aggregates. Furthermore, the density and thermal conductivity of concrete also decreased when plastic wastes were used as a replacement by up to 75%. Adnan and Dawood [18] found that there was an approximately 25% decrease in the splitting tensile strength of concrete when sand was substituted by plastic waste by up to 10.0%, compared to concrete without plastic waste. Ullah et al. [19] found that compressive strength, splitting tensile strength, and unit weight of concrete containing electronic waste reduced by 13.6, 20.5, and 13.9%, respectively, for a replacement ratio of up to 20%. In addition, Shaker et al. [20] studied the replacing sand with PET waste in high-strength concrete and found that by using 50% of PET waste, the density and thermal conductivity of concrete became less than 2000 kg/m^3 and 0.71 W/m.K, respectively. Although the replacement of natural aggregate with plastic waste reduces the mechanical properties of mortar and concrete, the lower density and thermal conductivity of the resulting composites offer their alternative application as lightweight and thermal-resistant materials [21–23].

Geopolymer, an alternative material to cement, is an environmentally friendly binder due to its lower carbon dioxide emissions from the manufacturing process and lower natural resources consumption, while the compressive strength and durability are comparatively high [24–28]. Various agro-industrial wastes and by-products, such as fly ash, slag, and rice husk ash, can be used as raw materials for the production of geopolymer. Meanwhile, new raw materials have begun to be used in the production of geopolymer, such as perlite [29]. Furthermore, in an effort to improve the properties of geo-polymers, Celik [30] found that the addition of 5% recycled steel fibers from waste tire in the geopolymer mixture yielded compressive strength up to 53 MPa, while the reference was 26 MPa. Recently, several reports have shed light on the use of plastic wastes as partial substitutions in geopolymers. Lazorenko et al. [15] investigated the use of different forms of PET waste, including particles, flakes, and strips, as aggregates in geopolymer composites. The results

showed that, regardless of plastic shapes, the incorporation of PET waste resulted in a reduction in compressive strength, flexural strength, and splitting tensile strength of the geopolymer. However, PET waste in the form of particles had a less negative impact on mechanical strength due to its greater compaction than the other two forms of PET waste. Moreover, Wongkvanklom et al. [31] found that even though recycled plastic beads had a deleterious effect on the mechanical properties of geopolymer concrete, they could reduce the density and thermal conductivity, which are favorable properties for being a lightweight and thermal-resistant material. Therefore, similar to the case of cement, plastic wastes are a source of aggregates that can provide promising properties for geopolymers.

Furthermore, it has been known that geopolymer has a superior fire resistance property than ordinary Portland cement (OPC) because it contains less amount of calcium compounds than OPC [32]. Temperatures of 200 °C up to as high as 1000 °C could even enhance the compressive strength of the geopolymer due to additional geopolymerization and sintering effect [33,34]. Nevertheless, the compressive strength declined after exposure to higher temperatures because of the differences in the thermal expansion coefficients of the aggregates and the geopolymer matrix [35]. In the case of plastic-containing geopolymers, it was found that the studies on the residual strength after exposure to high temperatures were still limited. Therefore, it is interesting to investigate the durability of plastic-incorporating geopolymer in terms of its resistance to fire, which is the focus of this current study.

This work then aimed to use PVC plastic from bottle labels as a fine aggregate in geopolymer mortar. The mechanical and physical properties of the resulting material, including compressive strength, flexural strength, splitting tensile strength, density, porosity, water absorption, ultrasonic pulse velocity, thermal conductivity, and microstructure were investigated. In addition, the mechanical and physical properties of the material after exposure to elevated temperatures were also tested to assess its fire-resistant property. The findings in this study would provide a promising way to reuse non-recyclable PVC waste for the production of "green" materials.

2. Materials and Methods

2.1. Materials

The binder used in this study was fly ash from the Mae Moh power plant in the northern part of Thailand. It had a specific gravity of 2.24, and the percentage retained on a sieve No. 325 of 34.8%. The chemical compositions of fly ash are listed in Table 1. Alkali activators used in the experiment were sodium hydroxide (NaOH) and sodium silicate (Na_2SiO_3). Sodium hydroxide at a concentration of 10 molar was prepared by diluting 400 g NaOH flakes (98% purity) in 1 L of distilled water. Then, the solution was left to cool down at room temperature for 24 h. A commercial-grade sodium silicate solution consisting of 32.39% SiO_2, 13.44% Na_2O, and 54.17% H_2O by weight was used without any modification. River sand and bottle label waste aggregates (BLWA) were used as fine aggregates. River sand with a maximum size of 4.75 mm was soaked in water for at least 24 h and then air-dried to provide saturated surface dry (SSD) condition, according to the ASTM C128 [36] standard. BLWA (Figure 1) was derived from bottle labels that had been separated from plastic bottles and collected by a recycling site in Northeast Thailand. They were cleaned, dried, and shredded by a shredding machine. The physical properties of both types of fine aggregates are summarized in Table 2. The sieve analysis according to the ASTM C136 [37] standard was conducted to determine the particle size distribution of fine aggregates. Sieve size and cumulative passing of fine aggregates are listed in Table 3, in which the lower and upper limits following the ASTM C33 [38] standard were also shown. It is evidenced that almost 90% of BLWA were retained on sieve No. 16, while the natural fine aggregate exhibited a more evenly distributed particle size.

Table 1. Chemical composition of fly ash.

Composition	Percentage (%wt)
Al_2O_3	21.3
SiO_2	41.3
CaO	15.1
Fe_2O_3	11.9
MgO	2.5
K_2O	2.4
SO_3	2.5
LOI	0.7

Figure 1. (**a**) Bottle label waste (**b**) BLWA.

Table 2. Physical properties of fine aggregates.

Properties	Sand	BLWA
Specific gravity	2.59	1.12
Fineness modulus	2.74	3.73
Unit weight (kg/m^3)	1682	71
Water absorption (%)	0.63	-

Table 3. Sieve size and cumulative passing of fine aggregates.

Sieve Size (mm)	Cumulative Passing (%)		Lower Limit (%) ASTM C33 [38]	Upper Limit (%) ASTM C33 [38]
	Sand	BLWA		
4.75 (#4)	97.9	100.0	95	100
2.36 (#8)	90.1	94.5	80	100
1.18 (#16)	76.7	21.9	50	85
0.60 (#30)	49.0	8.3	25	60
0.30 (#50)	11.4	1.6	10	30
0.15 (#100)	1.4	0.4	2	10

The BLWA were subjected to thermogravimetric analysis (TGA) to determine their thermal stability indicating their type of plastic as shown in Figure 2. The results illustrated that the thermal degradation of BLWA started at a temperature of approximately 250 °C with two-stage decomposition. The first degradation stage of BLWA occurred at a temperature of 190–350 °C due to the decomposition of chlorine in the form of a hydrochloric compound [39]. Then, at a temperature in the range of 420–550 °C, the second degradation in which the PVC backbone is broken into carbon dioxide and water occurred [40]. After both stages of thermal degradation, the total weight loss of the BLWA was approximately 85%, and the remaining weight was 15%. This was attributed to the inorganic additive added to PVC during the manufacturing process [40]. This result agreed with the work of

Yu et al. [41], suggesting that the thermal degradation of PVC was lower than polyethylene (PE), polypropylene (PP), PET, and polystyrene (PS). In addition, other types of plastic showed one-stage decomposition, while PVC exhibited two-stage decomposition. A similar TGA curve of PVC was also reported by Merlo et al. [42] and Suresh et al. [40]. Therefore, BLWA used in this study were PVC type.

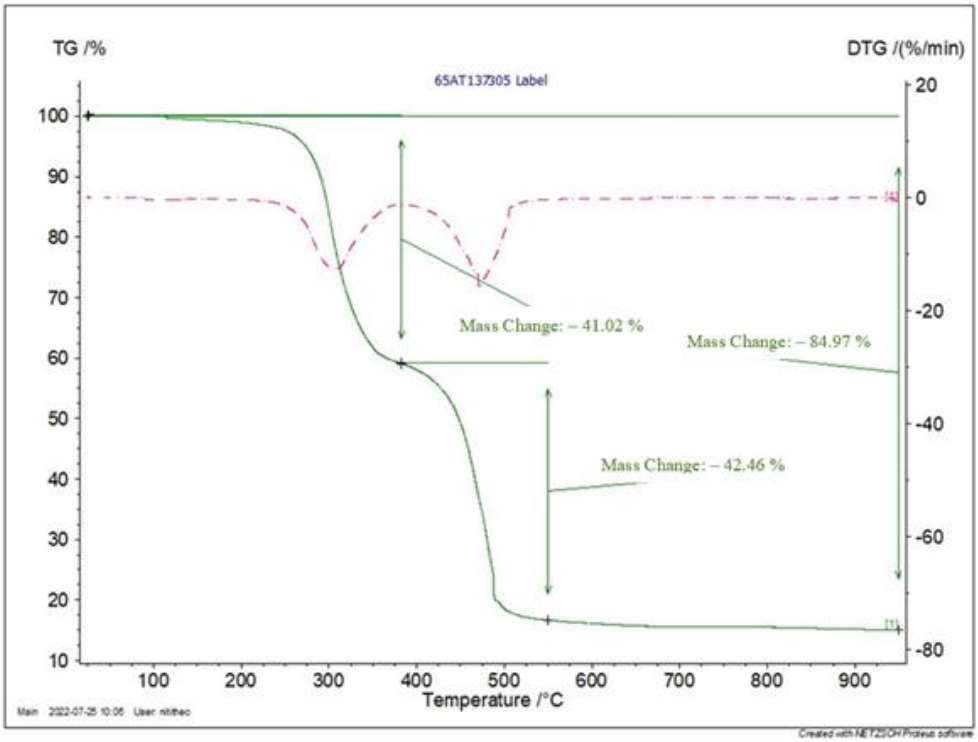

Figure 2. TGA curve of BLWA.

2.2. Mix Proportion

The geopolymer mortar was prepared with an alkali-to-binder ratio of 0.70, a fine aggregate-to-binder ratio of 2.75, and a NaOH:Na_2SiO_3 ratio of 1.00, which this mix proportion is recommended by Chindaprasirt et al. [43] for relatively high compressive strength mortar. The substitution of river sand with BLWA was carried out at the following ratios: 0, 5, 10, 15, and 20% by volume, in which the resulting materials were designated as LG00, LG05, LG10, LG15, and LG20, respectively. Due to the absence of admixtures, the maximum replacement of sand by BLWA in geopolymer mortar without compromising the workability was 20% by volume. The mix proportions of geopolymer mortar are listed in Table 4.

Table 4. Mix proportion of geopolymer mortar (kg/m^3).

Mix	FA	NS	NH	RS	BLWA
LG00	453	159	159	1246	-
LG05	453	159	159	1184	26
LG10	453	159	159	1121	53
LG15	453	159	159	1059	80
LG20	453	159	159	997	106

To prepare geopolymer mortar, fly ash was mixed with 10 M NaOH solution for 5 min. Fine aggregate was then added and mixed for 5 min. Then, Na_2SiO_3 solution was added and mixed further for 5 min. The geopolymer mortar mixture was cast into an acrylic mold and then covered by clingfilm to prevent moisture loss. The specimens were cured in an electric oven at 60 °C for 48 h. Afterward, the specimens were demolded

and cured in a humidity chamber with 50% relative humidity (RH) at a temperature of 22 °C until the testing age of 7 days. Geopolymer mortar specimens prepared with different mix proportions are shown in Figure 3, which showed a significant surface change from the sample without plastic used (LG00) on the left to the sample with the highest amount of plastic waste (LG20) on the right. The pictures showed that LG15 and LG20 specimens showed relatively more porous surfaces than those of the other specimens. It was also observed that the BLWA were evenly distributed throughout the LG20 specimen without segregation.

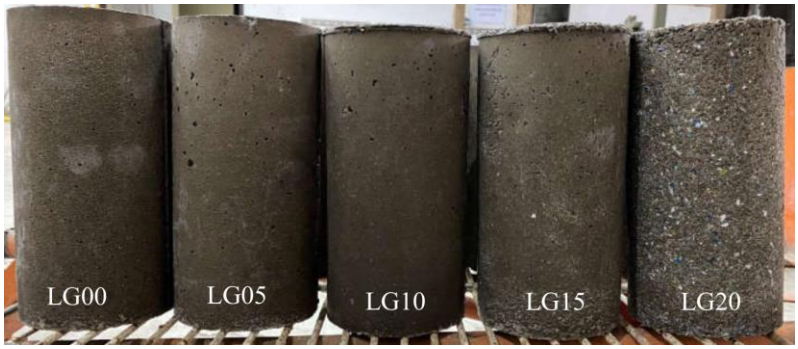

Figure 3. Geopolymer mortar specimens.

2.3. Testing

2.3.1. Fresh Properties

The workability of the fresh geopolymer mortar was determined by the flow table conforming to the ASTM C1437 [44] standard. The fresh mortar was also tested for setting time by using a Vicat apparatus according to ASTM C807 [45].

2.3.2. Physical Properties

Physical properties of geopolymer mortar, including density, porosity, water absorption, ultrasonic pulse velocity (UPV), and thermal conductivity, were tested on the 100 mm cube specimens. The density, porosity, and water absorption tests were carried out according to the ASTM C642 [46] standard. Thermal conductivity was tested using an ISOMET 2114 apparatus [47] in compliance with the ASTM D5930 [48] standard. Non-destructive UPV test was performed according to the ASTM C597 [49] standard.

2.3.3. Mechanical Properties

The 50 mm cube specimens were tested for compressive strength as per ASTM C109 [50] standard. Three-point bending test was performed on a 40 × 40 × 160 mm prism specimen to assess flexural strength according to the ASTM C348 [51] standard. The cylinder specimens with a diameter of 100 mm and a height of 200 mm were tested for splitting tensile strength as per ASTM C496 [52] standard.

2.3.4. Fire Resistivity

Fire resistivity tests were performed on a control geopolymer mortar (LG00) and LG10 mortar with temperatures of 25 °C (room temperature), 300, 600, and 900 °C. The specimens were placed and arranged in an electric furnace as shown in Figure 4. The heating process was run as described in the previous works [33,53]. Briefly, the heating rate was increased by 5 °C/min until reached the target temperature and then maintained temperature for 60 min. The specimens were then allowed to cool down to room temperature in an electric furnace before being tested for the following properties: compressive strength, residual strength, weight loss, density, porosity, water absorption, UPV, and thermal conductivity. All tests were carried out in triplicate.

Figure 4. Placement of the specimens in the electric furnace.

2.3.5. Scanning Electron Microscope (SEM)

Broken pieces of geopolymer mortars obtained from compressive strength tests were used for the observation of microstructures using a scanning electron microscope.

3. Results and Discussion

3.1. Flow Value

The flow values of geopolymer mortar containing BLWA are shown in Figure 5. The flow value of the control specimen (LG00) was 126%, while that of the geopolymer mortar containing BLWA decreased with increasing BLWA replacement ratio. The impaired fluidity of the fresh geopolymer mortar was due to the flaky and angular shape of BLWA in comparison to the river sand [54,55]. This finding is consistent with Ferreira et al. [56], which showed that spherical PET waste had a less negative effect on workability than flaky and angular-shaped PET. As can be seen in Figure 5, the LG15 and LG20 specimens, which had considerably low flow values, showed more porous surfaces and possibly a decline in the mechanical strengths of geopolymer mortar.

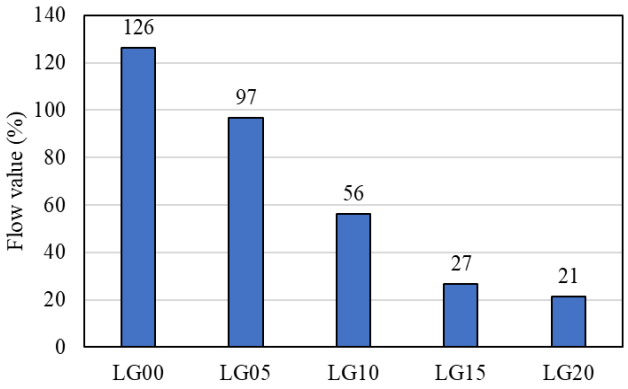

Figure 5. Flow values of geopolymer mortar containing BLWA.

3.2. Setting Time

The setting time of geopolymer mortars is shown in Figure 6. The initial setting time and final setting time of LG00, LG05, and LG10 were not significantly different. However, the setting time seems to be longer in LG15 and LG20, with the initial setting time and final setting time of 115 min and 156 min for LG15, and 126 min and 173 min for LG20. The presence of BLWA in the mixture did not hinder the geopolymerization in any way. The

longer setting time is due to the more porous structure with less geopolymer paste of LG15 and LG20.

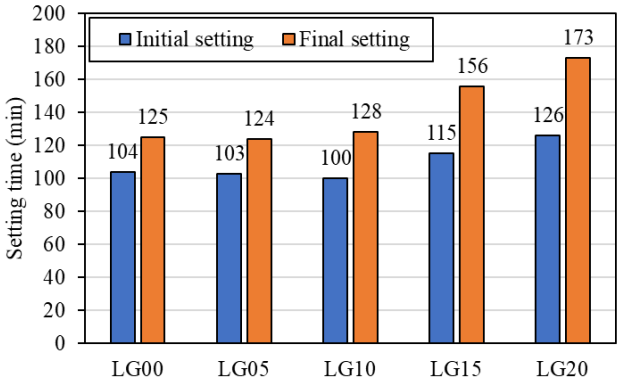

Figure 6. Setting time of geopolymer mortar containing BLWA.

3.3. Dry Density, Porosity, Water Absorption, and Ultrasonic Pulse Velocity

Dry density, porosity, water absorption, and UPV of geopolymer mortar are shown in Table 5. The results indicated that the dry density of geopolymer mortar containing BLWA significantly decreased with increasing BLWA contents. The highest dry density of 1989 kg/m^3 was found in LG00, whereas a drop in density of 17% was found in LG20. This was because BLWA has a lower density than sand, resulting in a reduction in the density of the geopolymer mortar. This finding agreed with other previous research showing that the incorporation of plastic aggregates in the mixture led to a reduction in the dry density of the cementitious composites.

Table 5. Dry density, porosity, water absorption, and ultrasonic pulse velocity of geopolymer mortar containing BLWA.

Mix	Density (kg/m^3) (STD .dev)	Porosity (%) (STD .dev)	Water Absorption (%) (STD .dev)	Ultrasonic Pulse Velocity (m/s) (STD .dev)
LG00	1989 (4.1)	20.6 (0.4)	7.7 (0.0)	3030 (190)
LG05	1819 (17.1)	26.9 (0.3)	9.4 (0.2)	2691 (44)
LG10	1732 (5.1)	27.5 (0.5)	9.8 (0.3)	2606 (70)
LG15	1696 (8.3)	27.9 (1.6)	10.1 (0.4)	2476 (132)
LG20	1645 (6.2)	30.4 (0.8)	10.7 (0.5)	2295 (96)

Moreover, there was evidence indicating that it is not only the type and density of the plastic aggregate but also the porosity of the materials that influenced the density of the composites [17,19]. Kaur and Pavia [57] showed that the reduction in dry density of cement mortar containing 20% PET waste was higher than that of the mortar containing 20% PC waste, although PET (density of 1.36 g/cm^3) was denser than PC (density of 1.24 g/cm^3). These results noticeably suggested that other than the types and density of the plastic waste, the porosity of the composite also played an important role. The flaky and angular shape of the BLWA in this present study resulted in increased pores within the matrix due to difficulty in compaction. It should be noted that the density of all geopolymer mortars containing BLWA in this study meets the standard recommended by ACI 213R-14 [58], in which the dry density of structural lightweight concrete should be less than 1850 kg/m^3. Therefore, the replacement of natural fine aggregate with BLWA yielded a lightweight property to the geopolymer mortar.

Furthermore, the porosity of geopolymer mortar incorporated with BLWA was investigated. The results in Table 5 indicated that the porosity of geopolymer mortar increased with the increasing BLWA content. This was because the flaky and angular shape and poor particle size distribution of BLWA reduced the compact ability of the geopolymer

mortar. Moreover, the impermeability nature of BLWA caused the deposition of free water surrounding the BLWA particles, thus resulting in more pores in the interfacial transition zone between BLWA and the matrix [59]. As a result of increased porosity, water absorption of geopolymer mortar containing BLWA increased with an increasing replacement ratio. All of these results suggested that the partial substitution of BLWA as fine aggregate in geopolymer mortar led to a decrease in density and an increase in porosity and water absorption.

UPV is one of the techniques used to verify material integrity. The ultrasonic pulse travels faster when passing through a material with denseness and consistency [49]. The UPV of geopolymer mortar with partial substitution of BLWA at ratios of 0, 5, 10, 15, and 20% by volume were 3030, 2691, 2606, 2476, and 2295 m/s, respectively. This indicated that replacing sand with BLWA resulted in a reduction in UPV. This reduction is attributed to an increase in porosity within the matrix, which caused discontinuities impeding pulse motion. Furthermore, the sheet-like morphology of BLWA may act as a reflection, which can also interrupt the movement of the ultrasonic pulse [60–62].

3.4. Compressive, Flexural, and Splitting Tensile Strengths

The compressive, flexural, and splitting tensile strengths of geopolymer mortar are shown in Figures 7–9. Specimens after failure are also shown in Figure 10. The strengths of geopolymer mortar decreased with the increase in the substitution ratio of BLWA in the mixture. The compressive strengths of LG05, LG10, LG15, and LG20 were 26.3, 24.5, 18.8, and 11.5 MPa, respectively. For the highest substitution level, the compressive strength of geopolymer mortar containing BLWA was reduced by 59% compared to the control sample. This result was consistent with other previous research, which also suggested that a reduction in compressive strength was a result of low bond strength between plastic and the geopolymer paste [15,17,19,31,63,64]. Moreover, the hydrophobic nature of BLWA caused the free water to locate around them, which then reduced the adhesiveness between BLWA and the paste [59,65]. The significant difference in elastic modulus between plastic aggregate and geopolymer paste also resulted in an imbalanced modulus and thus led to the development of micro-crack causing a decrease in the compressive strength of the composite [66]. However, the obtained compressive strength of geopolymer mortar containing BLWA (up to 15% replacement) in this present study was higher than the required strength for structural lightweight concrete (17 MPa) as recommended by ACI 213R-14 [58].

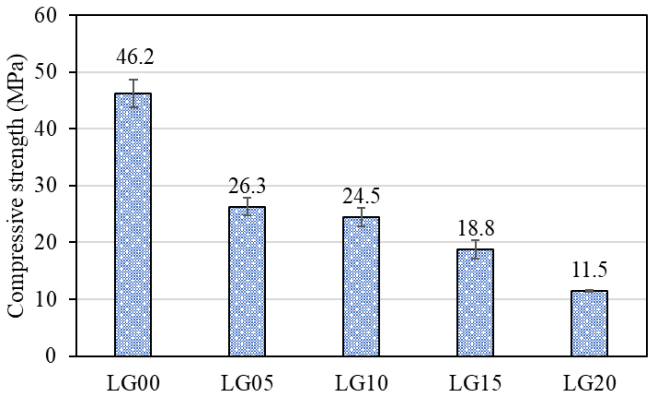

Figure 7. Compressive strength of geopolymer mortar containing BLWA.

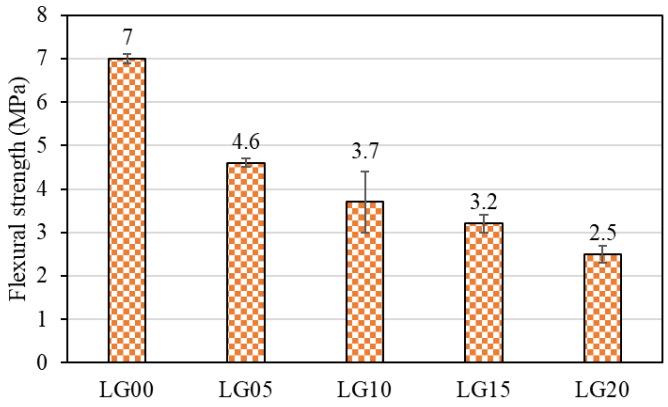

Figure 8. Flexural strength of geopolymer mortar containing BLWA.

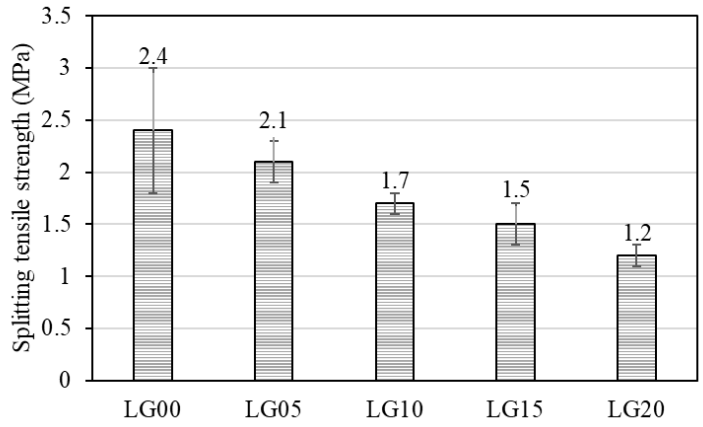

Figure 9. Splitting tensile strength of geopolymer mortar containing BLWA.

Figure 10. Specimens after failure.

When considering the compressive strength together with the dry density as shown in Figure 11, it was found that although the compressive strength of LG00 achieved the requirement for structural lightweight concrete, the dry density was higher than the specification. In contrast, LG20 had a satisfactory dry density, but its compressive strength was lower than the minimum limit. The replacement of sand with BLWA at a ratio of 5, 10, and 15% by volume in mixtures (LG05, LG10, and LG15, respectively) resulted in the composites with desirable properties, which achieved the requirement recommended by ACI 213R-14 [58] in both the compressive strength and the dry density, confirming that these mixtures could be used as structural lightweight concrete. Furthermore, the compressive strengths of LG05, LG10, and LG15 in a range of 18.8–26.3 MPa suggested that they are applicable for Type M masonry concrete (12.4 MPa), while LG20 (11.5 MPa) could be used as Type S (3.4 MPa) according to the ASTM C91 [67] standard. Moreover, the result also presented the strong relationship between compressive strength and dry density of geopolymer mortar containing BLWA with a correlation coefficient of as high as

0.9639. These findings offered the alternative use of geopolymer mortar containing BLWA as masonry work.

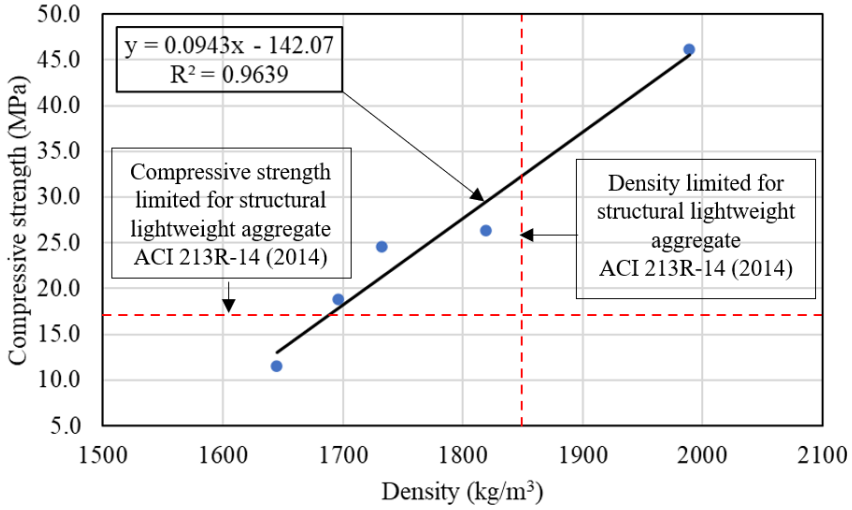

Figure 11. Relationship between density and compressive strength of geopolymer mortar containing BLWA compared with the limited for structural lightweight aggregate as ACI 213R-14 [58].

As seen in Figures 8 and 9, the tensile strengths, including flexural strength and splitting tensile strength, tended to decrease with an increase in BLWA contents. The flexural strength reduced from 7 MPa in LG00 to 2.6 MPa in LG20, while the splitting tensile strength reduced from 2.4 MPa (LG00) to 1.2 MPa (LG20). The reduction in flexural strength and splitting tensile strength was, similar to the case of compressive strength due to the weak adhesiveness between BLWA and the geopolymer matrix. However, it was found that a ratio of flexural strength to compressive strength and a ratio of splitting tensile strength to compressive strength of geopolymer mortar containing BLWA (LG05, LG10, LG15, and LG20) enhanced when compared to the control mortar (LG00). This explained that the use of BLWA in geopolymer mortar caused a less negative effect on flexural strength and splitting tensile strength than on compressive strength. This was also observed in Hannawi et al. [68], in which PET and polycarbonate (PC) were used in cement mortar as partial replacements of natural sand 0, 3, 10, 20, and 50% by volume. The results showed that the compressive strength of cement mortar was significantly decreased with more plastic waste aggregate in the mixture, whereas the flexural strength when PET and PC were used up to 20% replacement was still close to that of the control mixture. In addition, in Figure 10, the specimen with BLWA showed the ductile failure mode, in which after reaching the maximum tensile strength, the specimens were not broken or separated. On the other hand, the specimens without BLWA were brittle and were immediately broken after failure. Babu et al. [69] and Saikia and Brito [70] also found that an increase in plastic content in the mixture could cause a reduction in the brittleness of concrete due to the flexibility of the plastics, which allowed the specimen to behave as a more ductile material.

3.5. Thermal Conductivity

The thermal conductivity of geopolymer mortar is shown in Figure 12. The results indicated that the use of BLWA could improve the thermal-resistant properties of geopolymer mortar. The substitution by 5% of BLWA could cause a dramatic drop of approximately 28% in thermal conductivity when compared to the control geopolymer mortar (LG00). For the highest replacement ratio (LG20), the thermal conductivity of geopolymer mortar was 0.6841 W/m·K, which was 45% lower than that of LG00. This can be explained by the lower thermal conductivity of BLWA than that of the natural sand. Belmokaddem et al. [71] experimented with PVC, HDPE, and PP as an aggregate in concrete and found that the higher the replacement content of plastic, the lower the thermal conductivity of the concrete.

In addition, Senhadji et al. [72] reported a 17% reduction in the thermal conductivity of cement mortar containing 10% PVC waste from pipes compared with reference mortar. It should be noted that the drop in thermal conductivity of mortar containing 10% BLWA compared to LG00 was 30%, which was higher than their finding. Another reason for lower thermal conductivity is that BLWA-containing geopolymer mortar had greater porosity than the control one, in which the pore or air void has the lowest thermal conductivity compared to other geopolymer mortar components [73]. Reduced thermal conductivity is an advantageous property of lightweight materials because it favors the application of thermal insulation panels in buildings, which can help save energy consumption. According to RILEM LC 2 [74], an insulating material can be classified by the thermal conductivity of lower than 0.75 W/m·K. With LG20 having a thermal conductivity of 0.6841 W/m·K in this work, it therefore meets the standard and could be used as thermal-insulating material.

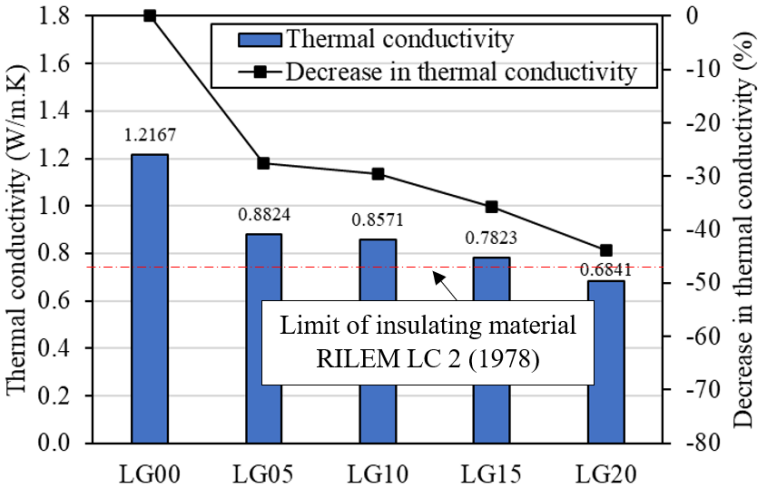

Figure 12. Thermal conductivity of geopolymer mortar containing BLWA compared with the limit of insulating material as RILEM LC 2 [74].

Figure 13 shows the relationship between UPV and the thermal conductivity of geopolymer mortar containing BLWA. The exponential equation with the correlation coefficient (R^2) of 0.988 indicated that the increase in thermal conductivity was strongly related to a higher value of UPV. The relationship is expressed as follows:

$$K = 0.1141e^{0.0008UPV}, \quad (1)$$

where K is thermal conductivity (W/m·K) and UPV is ultrasonic pulse velocity (m/s).

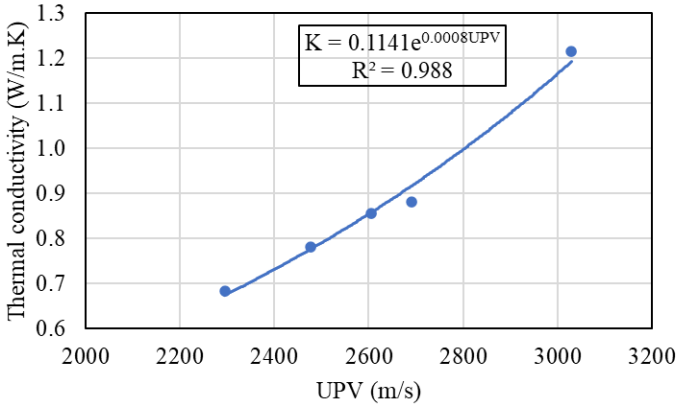

Figure 13. Relationship between UPV and thermal conductivity of geopolymer mortar containing BLWA.

According to Hacini et al. [75], an exponential relationship between UPV and thermal conductivity also showed a good correlation coefficient (R^2) of 0.7439. Thus, with the above equation, in addition to predicting the compressive strength from the UPV, it is also possible to estimate the thermal conductivity of geopolymer mortar from the UPV.

Moreover, Sengul et al. [76] stated that the thermal conductivity of concrete is strongly related to density. In addition to a reduction in density, more air voids in the matrix also enhanced the thermal insulating properties of mortar. The exponential relationship between the density and thermal conductivity of mortars in this study is plotted in Figure 14. A high correlation coefficient of 0.9686 confirmed a significant relationship between thermal conductivity and density. The empirical expression of this study is as follows:

$$K = 0.0553e^{0.0015D}, \quad (2)$$

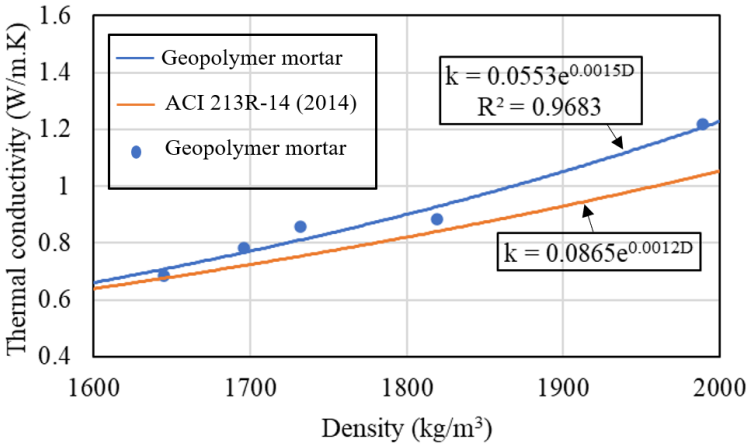

Figure 14. Relationship between density and thermal conductivity of geopolymer mortar containing BLWA compared with the equation of ACI 213R-14 [58].

The exponential relationship between density and thermal conductivity obtained in this study is consistent with the relationship computed by the ACI 213R-14 [58] recommendation, which is expressed as follows:

$$K = 0.0865e^{0.0012D}, \quad (3)$$

where K is thermal conductivity (W/m·K) and D is density (kg/m^3).

3.6. Fire Resistance

3.6.1. Visual Observation

Figure 15 shows LG00 and LG10 after exposure to different temperatures. At room temperature, the LG00 color was a dark gray which is typical of geopolymers. Due to the moisture loss, the color of LG00 was lightened after exposure to a higher temperature of 300 °C. The color of LG00 became reddish brown and light brown after exposure to temperatures of 600 and 900 °C. This phenomenon was also reported by Sarker et al. [77], Wongsa et al. [78], and Zhao and Sanjayan [79], which suggested that the color change was due to the high iron oxide content of fly ash. The discoloration of the LG10 after exposure to higher temperatures was similar to that of the LG00. However, there were black soot deposits on the surface of LG10 after exposure to temperatures of 300 and 600. This is possibly due to the incomplete combustion of BLWA. Although larger pores were observable on the surface of LG10 after exposure to elevated temperatures, which was caused by the gas pressure from the thermal degradation of the BLWA, thermally large cracks were not visible through the surface of the specimens. This ensures the durability of LG10 even after exposure to high temperatures.

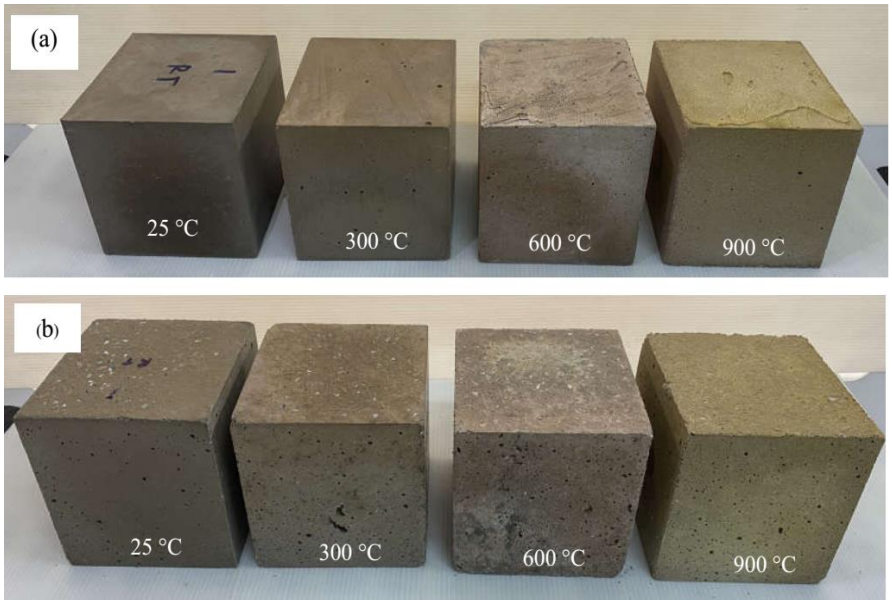

Figure 15. Specimens after exposure to elevated temperatures (**a**) LG00 (**b**) LG10.

Figure 16 illustrates the cracked surfaces of LG00 and LG10 after being tested for compressive strength. It was found that the matrix of LG00 varied markedly after exposure to elevated temperatures, wherein the denseness and homogeneity of the matrix were reduced. Meanwhile, apart from the alteration of the colors of the matrix and the external surface, the color of the sand also changed (Figure 16a,c,e,g). In the case of LG10, it was noticeable that BLWA dispersed throughout the specimen without segregation (Figure 16b). After exposure to the temperature of 300 °C, the BLWA thermally decomposed, and several dark brown spots on the cracked surface from the incomplete combustion of BLWA were observed (Figure 16d). The dark brown color became lighter after exposure to 600 °C (Figure 16f). At 900 °C, the highest calcined temperature in this study, the brown/black stains and the BLWA were not visible in the specimen (Figure 16h).

3.6.2. Compressive Strength

Figure 17 shows the compressive strength of control geopolymer mortar (LG00) and geopolymer mortar containing BLWA (LG10) before and after exposure to elevated temperatures. The compressive strength of LG00 tended to reduce after exposure to higher temperatures. The compressive strength of LG00 declined from 46.2 MPa at room temperature to 21.9 MPa and 7.9 MPa after exposure to 300 °C and 600 °C, respectively. The decrease in compressive strength was due to the thermal degradation of BLWA and the formation of cracks due to different thermal expansion coefficients between geopolymer paste and fine aggregate. In addition, the phase transition of fine aggregate from β-quartz to a larger volume of α-quartz resulted in the intensification of cracking [80]. This caused the lowest compressive strength of geopolymer mortar after being subjected to a temperature of 600 °C. Nevertheless, an elevated temperature of up to 900 °C led to a slight increase in the compressive strength of LG00. This finding agreed with Hager et al. [80], and Wongsa et al. [78], which showed a reduction in compressive strength of fly ash-based geopolymer mortar after calcination at 300–800 °C, but the strength was slightly increased after exposure to 800–1000 °C. Such enhancement of the compressive strength was suggested as a result of sintering and densification of the geopolymer matrix.

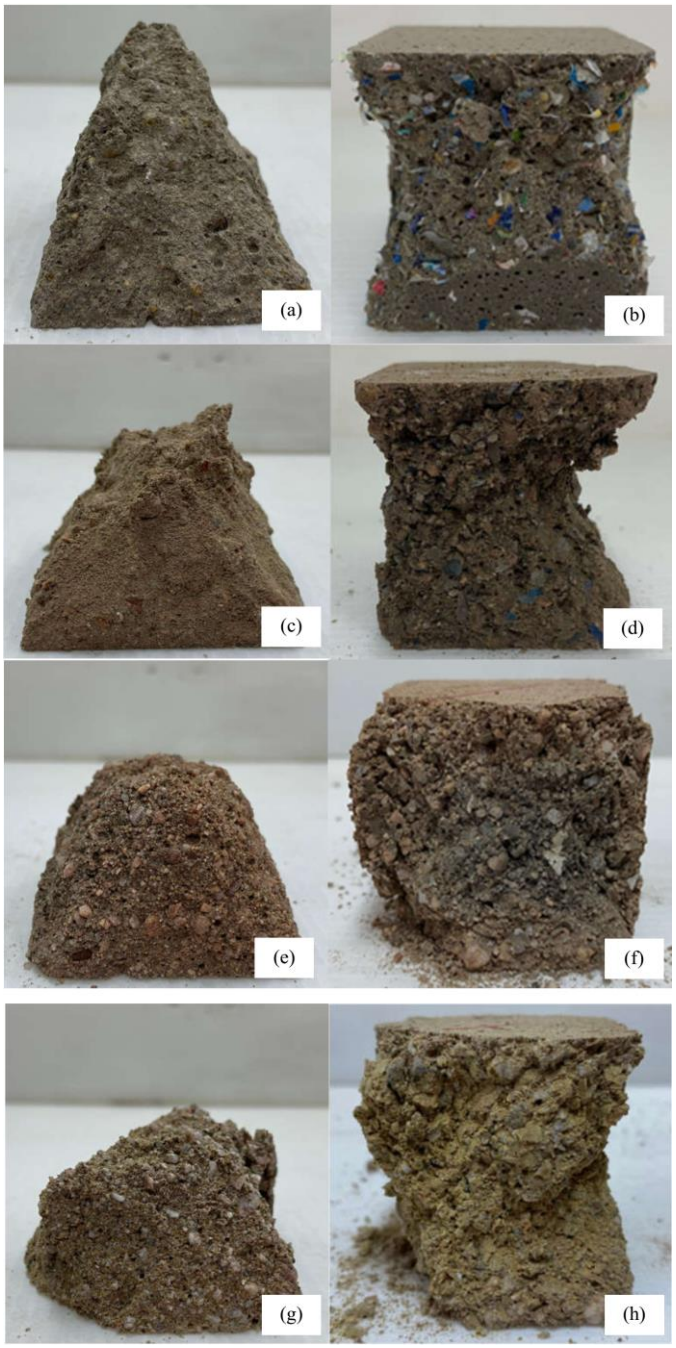

Figure 16. Specimens after exposure to elevated temperatures and being tested for compressive strength: (**a**) LG00-25 °C, (**b**) LG10-25 °C, (**c**) LG00-300 °C, (**d**) LG10-300 °C, (**e**) LG00-600 °C, (**f**) LG10-600 °C, (**g**) LG00-900 °C, and (**h**) LG10-900 °C.

Similar to the case of LG00, the compressive strength of geopolymer mortar containing BLWA (LG10) dramatically decreased after exposure to 300 °C and 600 °C. When the temperature was elevated to 900 °C, the compressive strength of LG10 was not significantly different from that of after exposure to 600 °C. This indicated that the temperature of 600 °C had the most negative impact on the compressive strength of LG10. This finding is consistent with Rickard et al.'s [81] work, which suggested that the critical exposure temperature for geopolymer composite with quartz sand was 600 °C.

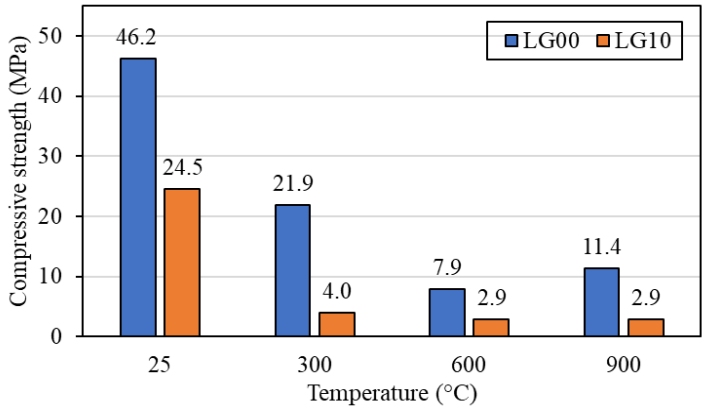

Figure 17. Compressive strength of LG00 and LG10 after exposure to elevated temperatures.

3.6.3. Residual Compressive Strength

The residual strengths of LG00 and LG10 after exposure to 300, 600, and 900 °C are shown in Figure 18. The results showed that the residual strength of LG10 was less than that of LG00 at all tested temperatures. This indicated that LG00 was more durable in high temperatures than LG10. This is due to the thermal degradation of BLWA at 600 °C as indicated by the TGA test. In addition, the difference in thermal expansion coefficients between the geopolymer paste and sand was lower than the difference between the paste and BLWA; thus, fewer pores and cracks were formed in LG00 than in LG10 after treating the composites with high temperature [82]. A larger reduction in compressive strength after exposure to high temperatures of the plastic-containing materials was also evidenced by Saxena et al. (2018), which reported that the strength of PET-containing concrete decreased up to ~47% after exposure to 600 °C, while a reduction in strength of reference concrete was only ~26%. Moreover, Correia et al. [83] also showed that the compressive strength of plastic-containing concrete was reduced more than that of the reference concrete after exposure to elevated temperatures. Although the incorporation of BLWA in geopolymer mortar reduced the durability at high temperatures, it is interesting that an increased temperature from 600 °C to 900 °C could no longer affect the strength of geopolymer mortar containing BLWA (LG10).

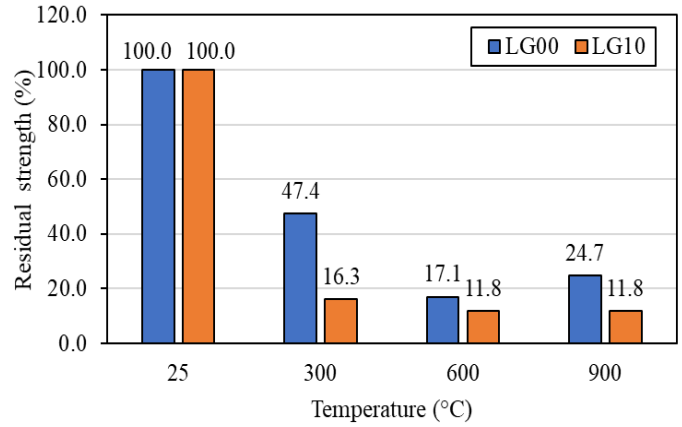

Figure 18. Residual compressive strength of LG00 and LG10 after exposure to elevated temperatures.

3.6.4. Weight Loss

Figure 19 shows the weight loss of geopolymer mortar after exposure to elevated temperatures. It was evidenced that both LG00 and LG10 experienced an increase in weight loss with increasing exposure temperatures. The largest loss of weight occurred at 300 °C, accounting for about 90% of the total weight loss. This is due to the loss of moisture in both weakly bound water and chemically bound water [80]. A slight increase

in weight loss of geopolymer mortar after exposure to higher temperatures is attributed to the decomposition of some geopolymerization products in the matrix [78]. A greater weight loss of LG10, when compared to LG00, was a result of the thermal decomposition of the BLWA in LG10. Moreover, a significant increase in weight loss of LG10 after exposure temperature increased from 300 °C to 600 °C correlated to the TGA analysis of BLWA, in which the degradation of BLWA continually occurred until 600 °C, a temperature beyond the melting point of BLWA. At a temperature of 900 °C, all BLWA completely burnt out, so the slight loss of weight was mainly due to the decomposition of other constituents in the geopolymer matrix.

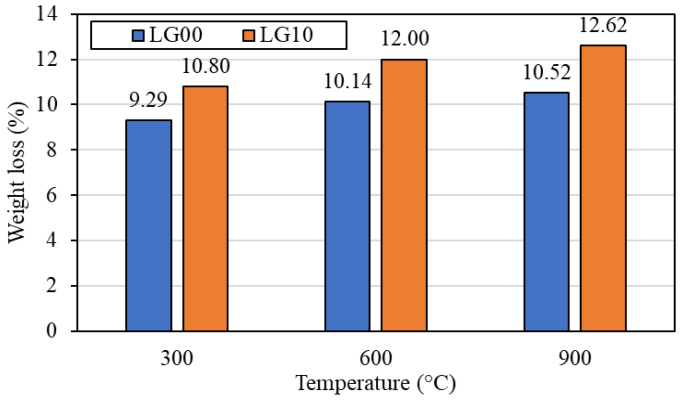

Figure 19. Weight loss of LG00 and LG10 after exposure to elevated temperatures.

3.6.5. Density, Porosity, Water Absorption, UPV, and Thermal Conductivity

Density, porosity, water absorption, UPV, and thermal conductivity of LG00 and LG10 after exposure to the temperature of 300, 600, and 900 °C were also investigated, as listed in Table 6. The results showed that the dry density of LG00 and LG10 decreased after the calcined temperature increased due to weight loss, and higher porosity occurred as a result of the thermal degradation of BLWA and different thermal expansion coefficients between the paste and aggregates. As the temperature rose from 25 °C to 300 °C, there was a huge weight loss of geopolymer mortars mainly due to moisture loss, while their volume did not change much. Therefore, a relatively high reduction in the density of geopolymer mortars was noticeable. At 600 °C, the dry density of geopolymer mortars continued to decrease, but the reduction rate was less than at 300 °C. When the temperature reached 900 °C, the weights of geopolymer mortars were still reduced together with a decrease in the volume of the materials due to densification and sintering, resulting in shrinkage of the geopolymer matrix. Thus, the density of geopolymer mortars slightly decreased further when compared to that of at 600 °C.

The porosity of LG00 and LG10 increased with increasing temperatures up to 600 °C. In the case of LG00, the phase change of sand due to high temperature could intensify the volume of microcracks, resulting in increased porosity. Differently, a larger pore volume within the matrix of LG10 was mainly due to the thermal degradation of BLWA, resulting in increased porosity. At 900 °C, sintering effects caused the geopolymer matrix to be denser, and thus porosity was reduced in LG00. Nevertheless, such an effect was not prominent in the case of LG10 since the degradation of BLWA left more pores than the sintering could repair. Likewise, an increase in water absorption of LG00 and LG10 was found when exposed to higher temperatures due to an increase in porosity. The higher porosity of the specimens brought about the absorption of water more readily. Moreover, when the temperature increased to 900 °C, large porosity caused a reduction in water absorption of both materials.

Table 6. Density, porosity, water absorption, UPV, and thermal conductivity of LG00 and LG10 after exposure to elevated temperatures.

Mix	Temperature (°C)	Properties				
		Density (kg/m^3)	Porosity (%)	Water Absorption (%)	UPV (m/s)	Thermal Conductivity (W/m·K)
LG00	25	1989	20.6	7.7	3030	1.2167
LG00	300	1953	26.1	10.0	1554	1.0469
LG00	600	1914	27.0	10.4	626	0.7472
LG00	900	1902	25.9	10.2	725	0.7641
LG10	25	1732	27.5	9.8	2606	0.8571
LG10	300	1653	34.8	12.3	1123	0.7021
LG10	600	1634	36.6	14.0	529	0.5789
LG10	900	1623	36.6	13.9	510	0.5129

It was clear that elevated temperatures induced more formation of voids and microcracks within the geopolymer matrix, thus resulting in a reduced density, higher porosity, increased water absorption, and lowered compressive strength. These voids and microcracks created a discontinuous matrix, which also reduced the UPV value and thermal conductivity. This is because the air inside voids within the matrix had a relatively low thermal conductivity. However, the porosity of LG00 decreased and the compressive strength slightly increased after exposure to 900 °C due to the sintering process. Therefore, UPV and thermal conductivity of LG00 slightly increased at this temperature. On the other hand, the UPV and thermal conductivity of LG10 experienced no significant change after heating at 900 °C. This suggested that the increase in temperature to 900 °C did not have an additional effect on the geopolymer mortar containing BLWA.

3.6.6. SEM Image

SEM images of LG00 and LG10 before and after exposure to elevated temperatures are shown in Figure 20. In the cases of LG00 (Figure 20a) and LG10 (Figure 20b) before calcination, the microstructures of geopolymer mortars appeared homogenous and dense, with some unreacted fly ash and microcracks. The BLWA and natural aggregates adhered well to the geopolymer paste (Figure 20b). but a large gap between BLWA and the paste was observable (at 500× magnification) in the interfacial transition zone between the paste and the aggregates. This evidenced poor bondings between BLWA and the paste, which is probably the main cause of the strength deterioration of this material.

After being exposed to 300 °C, voids and microcracks were more pronounced and became connected in both LG00 and LG10. The presence of BLWA in the mixture can cause more voids after thermal exposure, thus more severe damage occurred to the microstructures of LG10 than to that of LG00. In addition, Figure 20d illustrates the microstructures of LG10 after exposure to 300 °C showed the discretion of thin sheets of the thermally decomposed BLWA scattering on the mortar's cracked surface. This suggested that the thermal alteration of LG10 microstructures led to a decrease in residual strength after calcination since the non-uniform distribution of the impaired BLWA was unable to sustain the compression loads.

Microstructures of the control geopolymer mortar and the geopolymer mortar containing BLWA after being exposed to 600 °C are shown in Figure 20e,f, respectively. At this temperature, the geopolymer paste was extensively decayed, revealing more voids and microcracks. Moreover, the interfacial transition zone between sand and geopolymer paste was larger than its original condition before incineration, resulting from the transformation of sands after expansion leading to a reduced bonding between sand and the binder, which caused a reduction in mechanical strength.

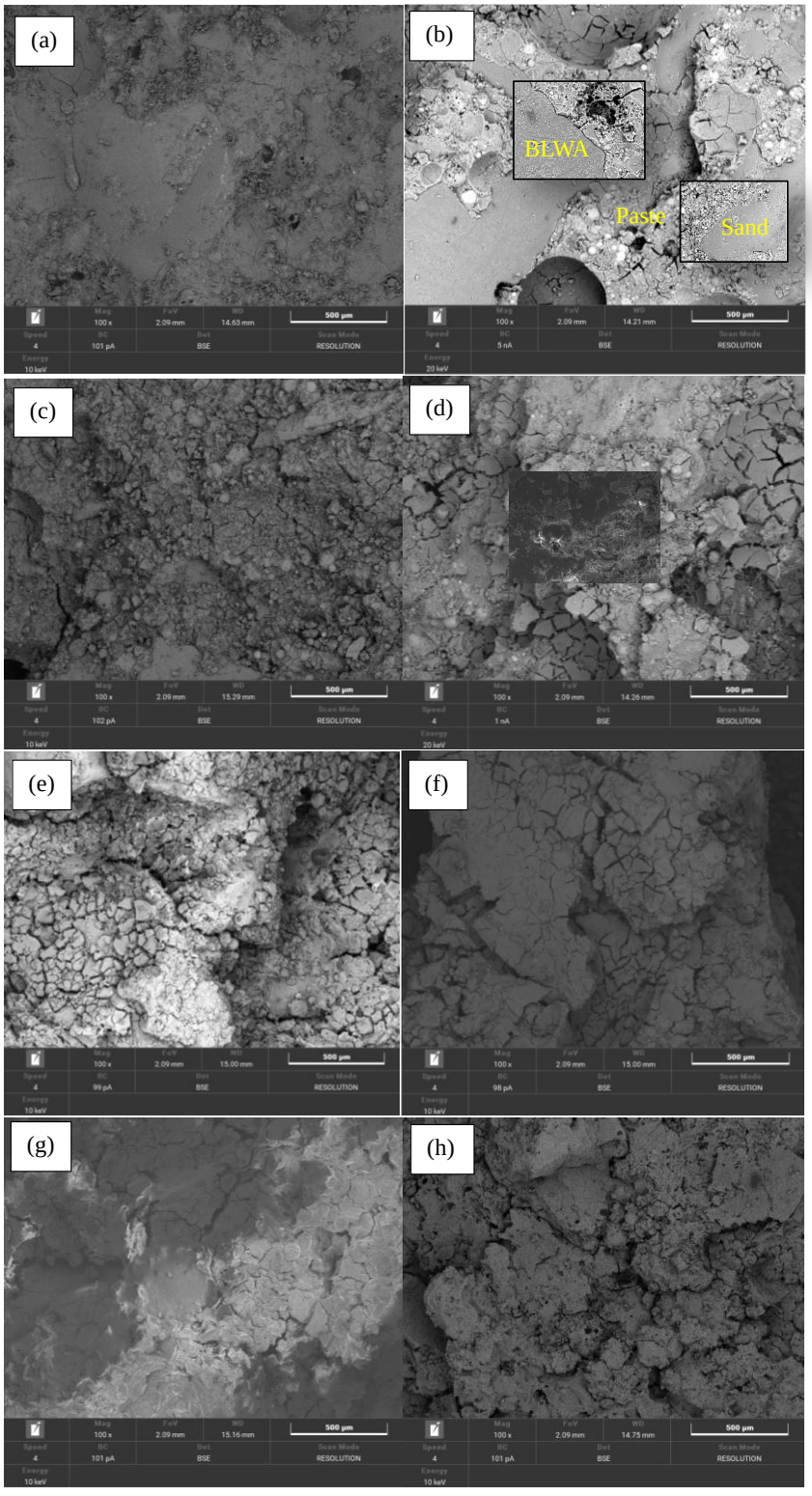

Figure 20. Microstructure of mortars: (**a**) LG00-25 °C, (**b**) LG10-25 °C, (**c**) LG00-300 °C, (**d**) LG10-300 °C, (**e**) LG00-600 °C, (**f**) LG10-600 °C, (**g**) LG00-900 °C, and (**h**) LG10-900 °C.

After the calcined temperature reached 900 °C, LG00 (Figure 20g) and LG10 (Figure 20h) showed changes in microstructures due to sintering and densification processes. Although porosity and microcracks were visible, the number of voids and microcracks in the paste was reduced. Some areas of the paste were more homogeneous and denser than the paste at 600 °C. The edges of the unreacted fly ash particles were less obvious, which were likely

to better blend in with the paste. These alterations contributed to a slight increase in the compressive strength of LG00. In addition, the healing of microcracks was more noticeable in LG00 when compared to LG10. This evidenced that sintering effects resulted in a more homogeneous matrix of the geopolymer mortar both with and without BLWA.

4. Conclusions

This work investigated the effects of replacing natural fine aggregates with PVC waste derived from bottle labels (BLWA) at 0–20% by volume. The mechanical, physical, and durability properties of the geopolymer mortars were comprehensively tested. The results can be summarized as follows:

1. The mechanical strength decreased with increasing BLWA contents. This reduction was due to weaker and lower bonding of BLWA with the geopolymer paste than those of natural fine aggregates. Note that although the compressive strength of geopolymer mortar containing BLWA was reduced, it met the requirement for use in masonry work. In addition, the use of a higher volume of BLWA could improve the ductility of geopolymer mortar.
2. The porosity and water absorption significantly increased due to increased voids at the interface between BLWA and the paste.
3. The compressive strength of 0% BLWA (LG00) and 10% BLWA (LG10) reduced with increasing exposure temperatures (300, 600, and 900 °C). The largest reduction in strength was observed at the temperature of 600 °C, considered a critical exposure temperature for this material.
4. The loss of weight and compressive strength of LG10 after exposure to elevated temperatures were higher than that of LG00 due to the thermal decomposition of BLWA. Interestingly, LG10 could maintain its weight and strength after exposure to 900 °C.
5. The increase in the substitution content of BLWA decreased the density and thermal conductivity of geopolymer mortar, which favored the use of BLWA for manufacturing eco-friendly lightweight geopolymer mortars with thermal-insulating properties.
6. The substitution of sand with BLWA 10% by volume in geopolymer mortar is the most suitable for engineering application, considering workability, physical and mechanical properties, and the amount of plastic waste reused in the mixture.

Author Contributions: Conceptualization, R.K. and V.S.; methodology, R.K. and V.S.; validation, A.W., J.E., P.S., and P.C.; investigation, R.K. and A.W.; resources, V.S.; data curation, R.K.; writing—original draft preparation, R.K.; writing—review and editing, J.E., P.S., V.S., and P.C.; supervision, V.S.; funding acquisition, V.S. All authors have read and agreed to the published version of the manuscript.

Funding: This research was funded by the Fundamental Fund of Khon Kaen University. The research on "The effect of waste materials powder on fly ash geopolymer properties" has received funding support from the National Science, Research and Innovation Fund (NSRF).

Data Availability Statement: Research data presented in this study are available on request from the corresponding author.

Conflicts of Interest: The authors declare no conflict of interest.

References

1. PlasticsEurope. *Plastics—The Facts 2016: An Analysis of European Plastics Production, Demand and Waste Data*. [Online] 2016. Available online: https://www.plasticseurope.org/wp-content/uploads/2021/10/2016-Plastic-the-facts.pdf (accessed on 20 August 2020).
2. Richens, J. *Plastics and Sustainability: A Valuation of Environmental Benefits, Costs and Opportunities for Continuous Improvement*; The American Chemistry Council (ACC): Washington, DC, USA, 2016.
3. EPA. *Advancing Sustainable Materials Management: Facts and Figures Report*; United States Environmental Protection Agency: Washington, DC, USA, 2019.
4. Awoyera, P.O.; Adesina, A. Plastic wastes to construction products: Status, limitations and future perspective. *Case Stud. Constr. Mater.* **2020**, *12*, e00330. [CrossRef]

5. Bridson, J.H.; Gaugler, E.C.; Smith, D.A.; Northcott, G.L.; Gaw, S. Leaching and extraction of additives from plastic pollution to inform environmental risk: A multidisciplinary review of analytical approaches. *J. Hazard. Mater.* **2021**, *414*, 125571. [CrossRef] [PubMed]
6. Khangale, U.B.; Ozor, P.A.; Mbohwa, C. A review of recent trends and status of plastics recycling in industries. *Eng. Appl. Sci. Res.* **2021**, *48*, 340–350.
7. Lithner, D.; Larsson, A.; Dave, G. Environmental and health hazard ranking and assessment of plastic polymers based on chemical composition. *Sci. Total Environ.* **2011**, *409*, 3309–3324. [CrossRef] [PubMed]
8. Oliveira, M.; Almeida, M.; Miguel, I. A micro(nano)plastic boomerang tale: A never ending story? *TrAC Trends Anal. Chem.* **2019**, *112*, 196–200. [CrossRef]
9. Zhang, K.; Hamidian, A.H.; Tubic, A.; Zhang, Y.; Fang, J.K.H.; Wu, C.; Lam, P.K.S. Understanding plastic degradation and microplastic formation in the environment: A review. *Environ. Pollut.* **2021**, *274*, 116554. [CrossRef]
10. Freedonia Group. *World Construction Aggregates—Industry Report*. [Online] 2019. Available online: https://www.freedoniagroup.com/industry-study/global-construction-aggregates-3742.htm (accessed on 21 July 2021).
11. Celik, A.I.; Ozkilic, Y.O.; Zeybek, O.; Karalar, M.; Qaidi, S.; Ahmad, J.; Burduhos-Nergis, D.D.; Bejinariu, C. Mechanical Behavior of Crushed Waste Glass as Replacement of Aggregates. *Materials* **2022**, *15*, 8093. [CrossRef]
12. Basaran, B.; Kalkan, I.; Aksoylu, C.; Ozkilic, Y.O.; Sabri, M.M.S. Effect of Waste Powder, Fine and Coarse Marble Aggregates on Concrete Compressive strength. *Sustainability* **2022**, *14*, 14388. [CrossRef]
13. Bamigboye, G.; Tarverdi, K.; Adigun, D.; Daniel, B.; Okorie, U.; Adediran, J. An appraisal of the mechanical, microstructure, and thermal characteristics of concrete containing waste PET as coarse aggregate. *Clean. Waste Syst.* **2022**, *1*, 100001. [CrossRef]
14. Kangavar, M.E.; Lokuge, W.; Manalo, A.; Karunasena, W.; Frigione, M. Investigation on the properties of concrete with recycled polyethylene terephthalate (PET) granules as fine aggregate replacement. *Case Stud. Constr. Mater.* **2022**, *16*, e00934. [CrossRef]
15. Lazorenko, G.; Kasprzhitskii, A.; Fini, E.H. Sustainable construction via geopolymer composites incorporating waste plastic of different sizes and shapes. *Constr. Build. Mater.* **2022**, *234*, 126697. [CrossRef]
16. Almeshal, I.; Tayeh, B.A.; Alyousef, R.; Alabduljabbar, H.; Mohamed, A.M. Eco-friendly concrete containing recycled plastic as partial replacement for sand. *J. Mater. Res. Technol.* **2020**, *9*, 4631–4643. [CrossRef]
17. Boucedra, A.; Bederina, M.; Ghernouti, Y. Study of the acoustical and thermo-mechanical properties of dune and river sand concretes containing recycled plastic aggregates. *Constr. Build. Mater.* **2020**, *256*, 119447. [CrossRef]
18. Adnan, H.M.; Dawood, A.O. Recycling of plastic box waste in the concrete mixture as a percentage of fine aggregate. *Constr. Build. Mater.* **2021**, *284*, 122666. [CrossRef]
19. Ullah, K.; Qureshi, M.I.; Armad, A.; Ullah, Z. Substitution potential of plastic fine aggregate in concrete for sustainable production. *Structures* **2022**, *35*, 622–637. [CrossRef]
20. Quidi, S.; Al-Kamaki, Y.; Hakeem, I.; Dulaimi, A.F.; Ozkilic, Y.; Sabri, M.; Sergeev, V. Investigation of the Physical-Mechanical Properties and Durability of High-Strength Concrete with Recycled PET as a Partial Replacement for Fine Aggregates. *Front. Mater.* **2023**, *10*, 1101146. [CrossRef]
21. Ghanem, H.; Chahal, S.; Khatib, J.; Elkordi, A. Flexural Behavior of Concrete Beams Reinforced with Recycled Plastic Mesh. *Buildings* **2022**, *12*, 2085. [CrossRef]
22. Nematzadeh, M.; Mousavimehr, M. Residual Compressive Stress–Strain Relationship for Hybrid Recycled PET–Crumb Rubber Aggregate Concrete after Exposure to Elevated Temperatures. *J. Mater. Civ. Eng.* **2019**, *31*, 04019136. [CrossRef]
23. Gopi, K.S.; Srinivas, T. Feasibility Study of Recycled Plastic Waste as Fine Aggregate in Concrete. In *E3S Web of Conferences*; EDP Sciences: Les Ulis, France, 2020.
24. Mesgari, S.; Akbarnezhad, A. Recycled geopolymer aggregates as coarse aggregates for Portland cement concrete and geopolymer concrete: Effects on mechanical properties. *Constr. Build. Mater.* **2020**, *236*, 117571. [CrossRef]
25. Si, R.; Guo, S.; Dai, Q.; Wang, J. Atomic-structure, microstructure and mechanical properties of glass powder modified metakaolin-based geopolymer. *Constr. Build. Mater.* **2020**, *254*, 119303. [CrossRef]
26. Tho-in, T.; Sata, V.; Boonserm, K.; Chindaprasirt, P. Compressive strength and microstructure analysis of geopolymer paste using waste glass powder and fly ash. *J. Clean. Prod.* **2017**, *172*, 2892–2898. [CrossRef]
27. Zhang, D.W.; Zhao, K.F.; Xie, F.; Li, H.; Wang, D. Rheology and agglomerate structure of fresh geopolymer pastes with different Ms ratio of waterglass. *Constr. Build. Mater.* **2020**, *250*, 118881. [CrossRef]
28. Kuri, J.C.; Hosan, A.; Shaikh, F.U.A.; Biswas, W.K. The Effect of Recycled Waste Glass as a Coarse Aggregate on the Properties of Portland Cement Concrete and Geopolymer Concrete. *Buildings* **2023**, *13*, 586. [CrossRef]
29. Acar, M.C.; Celik, A.I.; Kayabasi, R.; Sener, A.; Ozdoner, N.; Ozkilic, Y.O. Production of Perlite-Based-Aerated Geopolymer Using Hydrogen Peroxide as Eco-Friendly Material for Energy-Efficient Buildings. *J. Mater. Res. Technol.* **2023**, *24*, 81–99. [CrossRef]
30. Celik, A.I.; Ozkilic, Y.O. Geopolymer Concrete with High Strength, Workability and Setting Time Using Recycled Steel Wires and Basalt Powder. *Steel Compos. Struct.* **2023**, *46*, 689–707.
31. Wongkvanklom, A.; Posi, P.; Homwuttiwong, S.; Sata, V.; Wongsa, A.; Tanangteerapong, D.; Chindaprasirt, P. Lightweight geopolymer concrete containing recycled plastic beads. *Key Eng. Mater.* **2019**, *801*, 377–384. [CrossRef]
32. Strum, P.; Gluth, G.J.G.; Simon, S.; Brouwers, H.J.H.; Kühne, H.C. The effect of heat treatment on the mechanical and structural properties of one-part geopolymer-zeolite composites. *Thermochim. Acta* **2016**, *635*, 41–58. [CrossRef]

33. Payakaniti, P.; Chuewangkam, N.; Yensano, R.; Pinitsoontorn, S.; Chindaprasirt, P. Changes in compressive strength, microstructure and magnetic properties of a high-calcium fly ash geopolymer subjected to high temperature. *Constr. Build. Mater.* **2020**, *265*, 120650. [CrossRef]
34. Wattanasiriwech, S.; Nurgesang, F.A.; Wattanasiriwech, D.; Timakul, P. Characterisation and Properties of Geopolymer Composite Part 1: Role of Mullite Reinforcement. *Ceram. Int.* **2017**, *43*, 16055–16062. [CrossRef]
35. Abdulkareem, O.A.; Bakri, A.M.M.A.; Kamarudin, H.; Nizar, I.K.; Saif, A.A. Effects of elevated temperatures on the thermal behavior and mechanical performance of fly ash geopolymer paste, mortar and lightweight concrete. *Constr. Build. Mater.* **2014**, *50*, 377–387. [CrossRef]
36. *ASTM C128-17*; Standard Test Method for Density, Relative Density (Specific Gravity), and Absorption of Fine Aggregate. American Society for Testing and Materials: West Conshohocken, PA, USA, 2017; Annual Book of ASTM Standards, Volume 04.02.
37. *ASTM C136-17*; Standard Test Method for Sieve Analysis of Fine and Coarse Aggregates. American Society for Testing and Materials: West Conshohocken, PA, USA, 2017; Annual Book of ASTM Standards, Volume 04.02.
38. *ASTM C33-18*; Standard Specification for Concrete Aggregates. American Society for Testing and Materials: West Conshohocken, PA, USA, 2018; Annual Book of ASTM Standards, Volume 04.02.
39. Matuschek, G.; Milanov, N.; Kettrup, A. Thermoanalytical investigations for the recycling of PVC. *Thermochim. Acta* **2000**, *361*, 77–84. [CrossRef]
40. Suresh, S.S.; Mohanty, S.; Nayak, S.K. Composition analysis and characterization of waste polyvinyl chloride (PVC) recovered from data cables. *Waste Manag.* **2017**, *60*, 100–111. [CrossRef] [PubMed]
41. Yu, J.; Sun, L.; Ma, C.; Qiao, Y.; Yao, H. Thermal degradation of PVC: A review. *Waste Manag.* **2015**, *48*, 300–314. [CrossRef] [PubMed]
42. Merlo, A.; Lavagna, L.; Reira, D.S.; Pavese, M. Mechanical properties of mortar containing waste plastic (PVC) as aggregate partial replacement. *Case Stud. Construc. Mater.* **2020**, *13*, e00467. [CrossRef]
43. Chindaprasirt, P.; Chareerat, T.; Sirivivatnanon, V. Workability and Strength Of Coarse High Calcium Fly Ash Geopolymer. *Cem. Concr. Comp.* **2007**, *29*, 224–229. [CrossRef]
44. *ASTM C1437-15*; Standard Test Method for Flow of Hydraulic Cement Mortar. American Society for Testing and Materials: West Conshohocken, PA, USA, 2015; Annual Book of ASTM Standards, Volume 04.01.
45. *ASTM C807-20*; Standard Test Method for Time of Setting of Hydraulic Cement Mortar by Modified Vicat Needle. American Society for Testing and Materials: West Conshohocken, PA, USA, 2020; Annual Book of ASTM Standards, Volume 04.01.
46. *ASTM C642-13*; Standard Test Method for Density, Absorption, and Voids in Hardened Concrete. American Society for Testing and Materials: West Conshohocken, PA, USA, 2013; Annual Book of ASTM Standards, Volume 04.02.
47. Applied Precision Ltd. | Isomet 2114. Available online: https://www.appliedp.com/product/isomet/ (accessed on 10 February 2020).
48. *ASTM D5930-09*; Standard Test Method for Thermal Conductivity of Plastic by Means of a Transient Line-Source Technique. American Society for Testing and Materials: West Conshohocken, PA, USA, 2009; Annual Book of ASTM Standards, Volume 08.03.
49. *ASTM C597-16*; Standard Test Method for Pulse Velocity through Concrete. American Society for Testing and Materials: West Conshohocken, PA, USA, 2016; Book of Standards, Volume 04.02.
50. *ASTM C109/C109M-99*; Standard Test Method For Compressive Strength of Hydraulic Cement Mortars (Using 2-in or (50 mm) Cube Specimens). American Society for Testing and Materials: West Conshohocken, PA, USA, 2001; Annual Book of ASTM Standards, Volume 04.01.
51. *ASTM C348-97*; Standard Test Method for Flexural Strength of Hydraulic-Cement Mortars. American Society for Testing and Materials: West Conshohocken, PA, USA, 2001; Annual Book of ASTM Standards, Volume 04.01.
52. *ASTM C496/C496M-17*; Standard Test Method for Splitting Tensile Strength of Cylindrical Concrete Specimens. American Society for Testing and Materials: West Conshohocken, PA, USA, 2017; Book of Standards, Volume 04.02.
53. Zhang, H.; Kodur, V.; Qi, S.L.; Cao, L.; Wu, B. Development of metakaolin–fly ash based geopolymers for fire resistance applications. *Constr. Build. Mater.* **2014**, *55*, 38–45. [CrossRef]
54. Batayneh, M.; Marie, I.; Asi, I. Use of selected waste materials in concrete mixes. *Waste Manag.* **2007**, *27*, 1870–1876. [CrossRef]
55. Rahmani, E.; Dehestani, M.; Beygi, M.; Allahyari, H.; Nikbin, I. On the mechanical properties of concrete containing waste PET particles. *Constr. Build. Mater.* **2013**, *47*, 1302–1308. [CrossRef]
56. Ferreira, L.; De Brito, J.; Saikia, N. Influence of curing conditions on the mechanical performance of concrete containing recycled plastic aggregate. *Constr. Build. Mater.* **2012**, *36*, 196–204. [CrossRef]
57. Kaur, G.; Pavia, S. Physical properties and microstructure of plastic aggregate mortars made with acrylonitrile-butadiene-styrene (ABS), polycarbonate (PC), polyoxymethylene (POM) and ABS/PC blend waste. *J. Build. Eng.* **2020**, *31*, 101341. [CrossRef]
58. *ACI 213R-14*; Guide for Structural Lightweight-Aggregate Concrete. Reported by ACI Committee 213. ACI Manual of Concrete Practice Part I. American Concrete Institute: Farmington Hills, MI, USA, 2014.
59. Frigione, M. Recycling of PET bottles as fine aggregate in concrete. *Waste Manag.* **2010**, *30*, 1101–1106. [CrossRef] [PubMed]
60. Akçaözoglu, S.; Atis, C.D.; Akçaözoglu, K. An investigation on the use of shredded waste PET bottles as aggregate in lightweight concrete. *Waste Manag.* **2010**, *30*, 285–290. [CrossRef] [PubMed]
61. Ohemeng, E.A.; Ekolu, S.O. Strength prediction model for cement mortar made with waste LDPE plastic as fine aggregate. *J. Sustain. Cem.-Based. Mater.* **2019**, *8*, 228–243. [CrossRef]

62. Safi, B.; Saidi, M.; Aboutaleb, D.; Maallem, M. The use of plastic waste as fine aggregate in the self-compacting mortars: Effect on physical and mechanical properties. *Constr. Build. Mater.* **2013**, *43*, 436–442. [CrossRef]
63. Islam, M.J.; Meherier, M.S.; Islam, A.R. Effects of waste PET as coarse aggregate on the fresh and harden properties of concrete. *Constr. Build. Mater.* **2016**, *125*, 946–951. [CrossRef]
64. Latroch, N.; Benosman, A.S.; Bouhamou, N.-E.; Senhadji, Y.; Mouli, M. Physico-mechanical and thermal properties of composite mortars containing lightweight aggregates of expanded polyvinyl chloride. *Constr. Build. Mater.* **2018**, *175*, 77–87. [CrossRef]
65. Kou, S.; Lee, G.; Poon, C.; Lai, W. Properties of lightweight aggregate concrete prepared with PVC granules derived from scraped PVC pipes. *Waste Manag.* **2009**, *29*, 621–628. [CrossRef]
66. Zulkernain, N.H.; Gani, P.; Chuan, N.C.; Uvarajan, T. Utilisation of plastic waste as aggregate in construction materials: A review. *Constr. Build. Mater.* **2021**, *296*, 123669. [CrossRef]
67. *ASTM C91-18*; Standard Specification for Masonry Mortar. American Society for Testing and Materials: West Conshohocken, PA, USA, 2018; Book of Standards, Volume 04.01.
68. Hannawi, K.; Kamali-Bernard, S.; Prince, W. Physical and mechanical properties of mortars containing PET and PC waste aggregates. *Waste Manag.* **2010**, *30*, 2312–2320. [CrossRef]
69. Babu, K.G.; Babu, D.S. Behaviour of lightweight expanded polystyrene concrete containing silica fume. *Cem. Concr. Res.* **2003**, *33*, 755–762. [CrossRef]
70. Saikia, N.; Brito, J.D. Waste polyethylene terephthalate as an aggregate in concrete. *Mater. Res.* **2013**, *16*, 341–350. [CrossRef]
71. Belmokaddem, M.; Mahi, A.; Senhadji, Y.; Pekmezci, B.Y. Mechanical and physical properties and morphology of concrete containing plastic waste as aggregate. *Constr. Build. Mater.* **2020**, *257*, 119559. [CrossRef]
72. Senhadji, Y.; Siad, H.; Escadeillas, G.; Benosman, A.S.; Chihaoui, R.; Mouli, M.; Lachemi, M. Physical, Mechanical and Thermal Properties of Lightweight Mortars Containing Recycled Polyvinyl Chloride. *Constr. Build. Mater.* **2019**, *195*, 198–207. [CrossRef]
73. Iucolano, F.; Liguori, B.; Caputo, D.; Colangelo, F.; Cioff, R. Recycled plastic aggregate in mortars composition: Effect on physical and mechanical properties. *Mater. Des.* **2013**, *52*, 916–922. [CrossRef]
74. Rilem, L. Functional classification of lightweight concrete. *Mater. Struct.* **1978**, *11*, 281–283.
75. Hacini, M.; Benosman, A.S.; Tani, N.K.; Mouli, M.; Senhadji, Y.; Badache, A.; Latroch, N. Utilization and assessment of recycled polyethylene terephthalate strapping bands as lightweight aggregates in Eco-efficient composite mortars. *Constr. Build. Mater.* **2021**, *270*, 121427. [CrossRef]
76. Sengul, O.; Azizi, S.; Karaosmanoglu, F.; Tasdemir, M.A. Effect of expanded perlite on the mechanical properties and thermal conductivity of lightweight concrete. *Energy Build.* **2011**, *43*, 671–676. [CrossRef]
77. Sarker, P.K.; Kelly, S.; Yao, Z. Effect of fire exposure on cracking, spalling and residual strength of fly ash geopolymer concrete. *Mater. Des.* **2014**, *63*, 584–592. [CrossRef]
78. Wongsa, A.; Wongkvanklom, A.; Tanangteerapong, D.; Chindaprasirt, P. Comparative study of fire-resistant behaviors of high-calcium fly ash geopolymer mortar containing zeolite and mullite. *J. Sustain. Cem.-Based Mater.* **2020**, *9*, 307–321. [CrossRef]
79. Zhao, R.; Sanjayan, J.G. Geopolymer and Portland cement concretes in simulated fire. *Mag. Concr. Res.* **2011**, *63*, 163–173. [CrossRef]
80. Hager, I.; Sitarz, M.; Mroz, K. Fly-ash based geopolymer mortar for high-temperature application—Effect of slag addition. *J. Clean. Prod.* **2021**, *316*, 128168. [CrossRef]
81. Rickard, W.D.A.; Gluth, G.J.G.; Pistol, K. In-situ thermo-mechanical testing of fly ash geopolymer concretes made with quartz and expanded clay aggregates. *Cem. Concr. Res.* **2016**, *80*, 33–43. [CrossRef]
82. Saxena, R.; Siddique, S.; Gupta, T.; Sharma, R.K.; Chaudhary, S. Impact resistance and energy absorption of concrete containing plastic waste. *Constr. Build. Mater.* **2018**, *176*, 415–421. [CrossRef]
83. Correia, J.R.; Rima, J.S.; De Brito, J. Post-fire mechanical performance of concrete made with selected plastic waste aggregates. *Cem. Concr. Compos.* **2014**, *53*, 187–199. [CrossRef]